

RESEARCH

Open Access



Quercetin combined with shTERT induces apoptosis in ovarian cancer via the P53/Bax pathway, and RGD-MSN/QR/shTERT nanoparticles enhance the therapeutic efficacy

Guojie Chen^{1,2†}, Weiwei Song^{1,3†}, Xing Wang^{4†}, Guangyao Mao¹, Weifeng Hu^{1,3}, Rongrong Dou¹, He Zhu^{1,3}, Yongkang Zhang⁵, Xianhua Fu^{6*} and Mei Lin^{1,3*}

Abstract

Background Ovarian cancer (OC) is a highly malignant gynecological tumor with poor current treatment effects. Telomerase reverse transcriptase (TERT) is an important component of telomerase and plays an important role in the progression of ovarian cancer. Quercetin (QR) has been shown to inhibit the cell cycle and induce the apoptosis in various types of tumors. However, the mechanism of quercetin in ovarian cancer and whether it can be applied in the treatment of ovarian cancer has not been fully understood.

Results OC cells were intervened with QR in vitro and it was found that QR only inhibited the cell cycle but not induced cell apoptosis. By conducting network pharmacology, proteomics and TCGA-OV database analysis, we found that QR inhibited the cell cycle by binding to P53 and P21. However, in this study, overexpressed TERT in OC could bind to P53 and inhibit the binding of QR to P53, failing to induce tumor cell apoptosis. After TERT was knocked down, QR significantly suppressed the cell cycle of OC cells and induced apoptosis. To realize high drug delivery efficiency and drug targeting to improve the effect of inhibiting OC, we designed and prepared RGD-MSN/QR/shTERT nanoparticles for the combined administration of QR and shTERT. As confirmed by the in vivo experiments, RGD-MSN/QR/shTERT possessed good targeting ability and significant OC inhibiting effect, with no adverse reactions, and improved the survival benefits.

Conclusions This study demonstrated the mechanistic and therapeutic advantages of combining QR with shTERT in the treatment of OC. Based on this mechanism, we synthesized the novel nanoparticles (RGD-MSN/QR/shTERT) and verified the favorable OC inhibiting effect in vivo, providing a novel strategy for the treatment of OC.

Keywords Ovarian cancer, Quercetin, TERT, P53, Nanoparticle

[†]Guojie Chen, Weiwei Song and Xing Wang These authors contributed equally to this work.

*Correspondence:

Xianhua Fu

fxhua@163.com

Mei Lin

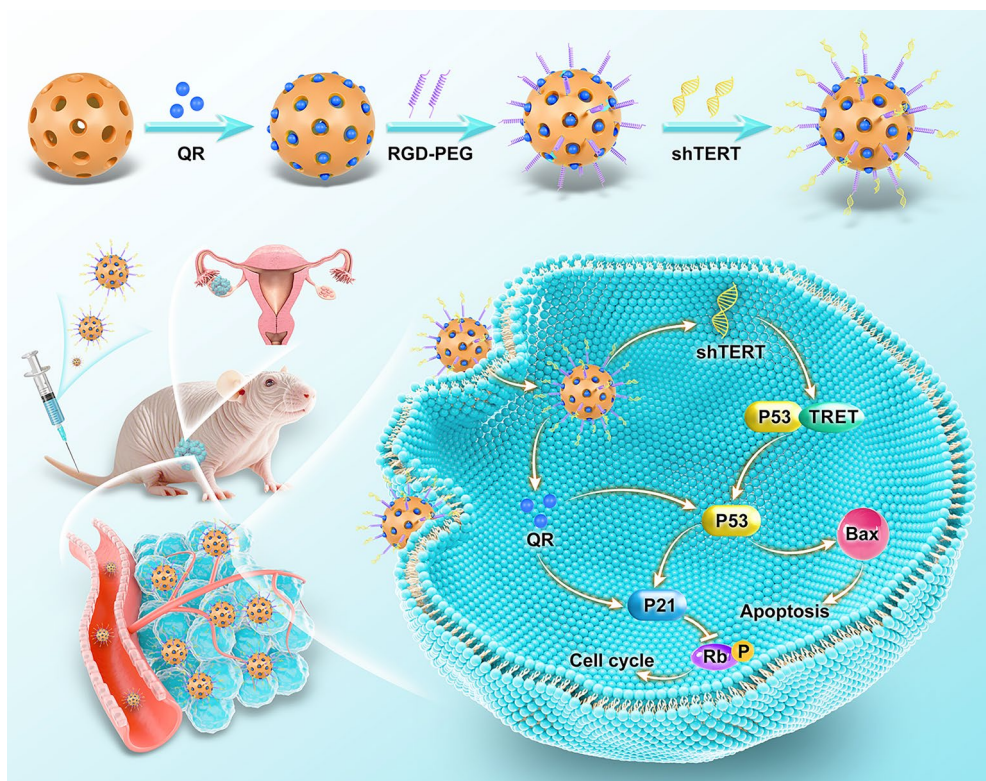
trylm@ntu.edu.cn

Full list of author information is available at the end of the article



© The Author(s) 2025. **Open Access** This article is licensed under a Creative Commons Attribution-NonCommercial-NoDerivatives 4.0 International License, which permits any non-commercial use, sharing, distribution and reproduction in any medium or format, as long as you give appropriate credit to the original author(s) and the source, provide a link to the Creative Commons licence, and indicate if you modified the licensed material. You do not have permission under this licence to share adapted material derived from this article or parts of it. The images or other third party material in this article are included in the article's Creative Commons licence, unless indicated otherwise in a credit line to the material. If material is not included in the article's Creative Commons licence and your intended use is not permitted by statutory regulation or exceeds the permitted use, you will need to obtain permission directly from the copyright holder. To view a copy of this licence, visit <http://creativecommons.org/licenses/by-nc-nd/4.0/>.

Graphical abstract



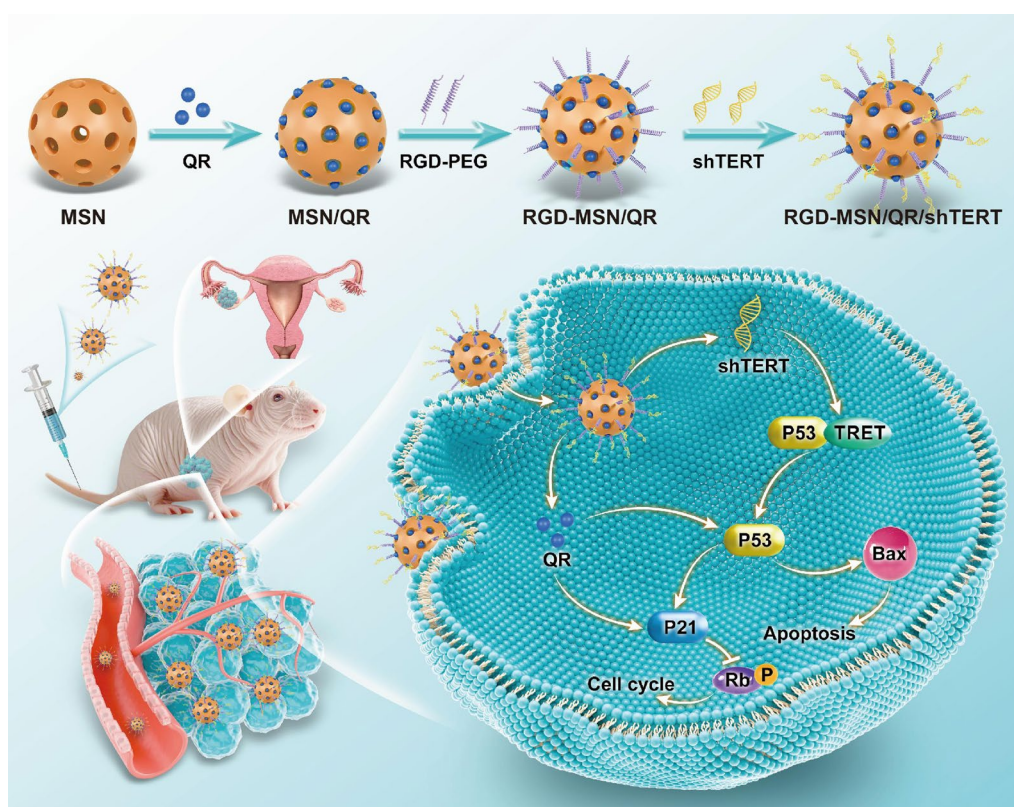
Introduction

The morbidity and mortality of ovarian cancer (OC), as a highly malignant tumor in the female reproductive system, show a continuously increasing trend, posing a major challenge to women's health [1]. At present, the only confirmed effective treatment options for OC are surgery and platinum-based chemotherapy [2]. However, more than half of OC patients still develop disease recurrence after treatment [3]. With the deepening of research, more and more natural compounds have been proven to have inhibitory effects on human cancer cells [4]. Compared with conventional chemotherapy, these natural compounds have fewer side effects, yet they are still associated with problems such as mediocre efficacy, poor targeting and low bioavailability [5]. Therefore, intensively exploring the molecular mechanism of natural compounds against cancer and attempting to overcome the above limitations may be an extremely promising treatment strategy for OC.

Flavonoids are widely distributed in plants [6] and play an important role in the body's defense system. Quercetin is a natural polyphenolic flavonoid commonly found in a variety of fruits and vegetables, with the most

important property being its antioxidant effect. In addition, quercetin can also be used for tumor prevention [7]. It has displayed good effects on inhibiting tumor cell cycle and inducing apoptosis in various cancers such as lung cancer, prostate cancer, liver cancer, breast cancer, colon cancer and cervical cancer [8]. Moreover, quercetin has a synergistic effect when used in combination with cisplatin and other chemotherapeutic drugs, which is expected to further improve the therapeutic results of traditional chemotherapy [9]. In view of the advantages of quercetin in the treatment of various types of tumors, we wonder whether it can be applied in the treatment of OC to overcome the numerous problems faced by the clinical treatment of OC.

Telomerase can ensure chromosome stability by maintaining the telomere length, thus delaying cell death and aging. Telomerase is composed of telomerase reverse transcriptase (TERT) and telomerase RNA (TR) [10]. Of them, TERT, as the catalytic subunit of telomerase, has the activity of reverse transcriptase, which can accelerate DNA replication, and plays a key role in cancer formation [11]. In addition to accelerating the cell cycle, TERT also participates in the interaction of



Scheme 1. Schematic illustration of RGD-MSN/QR/shTERT preparation and suppression of OC by activating the P53/Bax pathway

Wnt/ β -catenin and NF- κ B signaling pathways, inducing the malignant process of tumors [12]. Additionally, TERT can also interact with some transcription factors such as p53, WT1, CTCF and MZF-2, thereby inducing tumor occurrence [13]. Currently, there are relatively few therapeutic targets for OC. TERT is a highly expressed molecule in most tumors [14], can it be used as a therapeutic target for OC? Can it work synergistically with quercetin that also inhibits the cell cycle?

With the rapid development of nanomedicine, the nanocarrier drug delivery platform has emerged, which can not only achieve the efficient delivery of combined drugs, but also improve drug targeting, thus achieving the more accurate tumor therapy [15]. A number of natural compounds have the problems like poor stability, poor water solubility and low bioavailability, which have severely restricted their clinical application. Mesoporous silicon dioxide (MSN), as a functional nanoparticle, has great application potential, and research on its application in tumor has also increased rapidly due to the numerous studies in the field of biomedicine [16]. Due to the unique highly porous structure, adjustable pore size structure, easy surface functional modification, good biocompatibility and stability, MSN can

greatly improve bioavailability while enhancing drug safety [17]. MSN can also be assembled with polycations so that its surface is positively charged, which in turn effectively loads negatively charged nucleic acids through the potential electrostatic interactions. Furthermore, tumor cells or newly formed blood vessels can specifically express certain integrins such as $\alpha\beta 3$, which can bind to the RGD peptide with certain affinity, so carrying RGD peptide on nanocarriers can make drugs better target tumors.

This study aimed to further explore QR potential in OC treatment. Focused on the relationship among QR, TERT, and the P53 pathway, hypothesizing TERT's interference with QR-induced P53 activation. Moreover, a novel nanoparticle (RGD-MSN/QR/shTERT) was designed and prepared for the combined administration of quercetin and shTERT in vivo (Sch. 1). It provides a safe and effective strategy for the treatment of OC.

Materials and methods

Cell culture, compounds and cell transfection

The STR-validated OC cell lines ES-2 and SKOV-3 were purchased from Procell Life Science & Technology Co.,

Ltd. (China), and cultured within the Dulbecco's modified Eagle medium (DMEM) supplemented with 10% fetal bovine serum (FBS). Quercetin (QR) was purchased from MedChemExpress Co. (Cat# HY-18085A, USA). To silence TERT, ES-2 and SKOV-3 cells were transfected with a lentivirus shTERT plasmid chemically synthesized by Shanghai GenePharma Co., Ltd (China). The sequence of shTERT was as follows: 5'-CCATTTATTGAGACCAGACAT-3' #1; 5'-GACATGGAGAACAAGCTGTTT-3' #2; 5'-GCATTGGAATCAGACAGCACT-3' #3. The sequence of shNC was as follows: 5'-GTCATGGAGAAG AAGGTGTTT-3'.

Cell viability determination

To conduct cell viability assay, control and treated ES-2 and SKOV-3 cells were exposed to CCK-8 reagent (APExBio Corporation, USA) and cultured at 37 °C for 1 h, and the absorbance was measured using a microplate reader (BioTek, USA).

Colony formation assay

Control and treated ES-2 and SKOV-3 cells were evenly distributed in 6-well plates, with 1000 cells per well, and subsequently cultured at 37 °C for 21 days. The culture was subsequently fixed with 4% paraformaldehyde and stained with 0.1% crystal violet. Finally, the colony number was counted by a microscope (Nikon, Japan).

Cell cycle assay

The cell cycle was measured through flow cytometry. The control and treated ES-2 and SKOV-3 cells were evenly distributed in 6-well plates, with 1,000 cells per well, and the cells were incubated for 72 h. Next, the cells were washed thrice with PBS, stained in dark with PI reagent (Beyotime, China) at room temperature for 15 min, and the G0/G1 phase in cell cycle was evaluated using flow cytometry.

Apoptosis detection

Apoptosis was detected with a flow cytometer. The control and treated ES-2 and SKOV-3 cells were evenly distributed in 6-well plates, with 1,000 cells per well, and the cells were subsequently incubated for 72 h. After being washed thrice with PBS, the cells were stained with FITC-Annexin V reagent (Beyotime, China) and PI reagent (Beyotime, China) at room temperature in dark for 20 min, and flow cytometry was conducted to assess the apoptosis level.

TUNEL assay was performed to further measure the apoptosis level. In brief, control and treated ES-2

and SKOV-3 cells were cultured and fixed in 12-well plates, and later stained in dark with TUNEL reagent (Beyotime, China) for 1 h and subsequently with DAPI reagent (Beyotime, China) for 15 min at room temperature. Fluorescence signals were collected using a fluorescence microscope (Shanghai Zeicom Optical Instrument Co., Ltd, China) to assess the apoptosis level.

Western blotting assay

Total proteins were extracted from ES-2 and SKOV-3 cells using a RIPA lysis buffer containing phenylmethyl sulfonyl fluoride (Beyotime, USA). After quantification with the BCA protein assay kit (Beyotime, China), aliquots of proteins were separated through 10% SDS-PAGE and transferred to PVDF membranes. Following sealing with 5% skimmed milk powder at room temperature for 2 h, the membranes were incubated with TERT (ab289032; Abcam, UK), P53 (ab32509; Abcam, UK), P21 (ab109199; Abcam, UK), p-Rb (ab320747; Abcam, UK), Bcl-2 (ab182858; Abcam, UK) and Bax (ab32503; Abcam, UK) overnight at 4 °C. After washing, the membranes were further incubated with HRP-conjugated secondary antibodies at room temperature for 2 h, and the signals were visualized using a Pierce TM ECL Western blotting substrate (Thermo Fisher Scientific, USA).

Preparation of the nanomaterial

Cetyl Trimethyl Ammonium Bromide (CTAB) is a cationic surfactant that can bind to negatively charged nucleic acids (DNA, RNA) to form a complex. It can also adsorb on the surface of nanoparticles to form a protective film, preventing nanoparticles from agglomeration and stabilizing the dispersion system of nanomaterials, allowing nanomaterials to better perform their properties. CTAB, ethanol, ammonia and deionized water were mixed, stirred, and heated to 60 °C for 30 min. Afterwards, the TEOS solution was added to react for 2 h. Following repeated centrifugation and washing, the mixture was dispersed in the hydrochloric acid–ethanol solution, reacted at 60 °C for 14 h, and then centrifuged and washed repeatedly to obtain MSN 200 nm. Afterwards, MSN was mixed with quercetin overnight and centrifuged at 13000 rpm several times to obtain MSN/QR, which was later mixed with RGD-PEG overnight under stirring and centrifuged at 13000 rpm repeatedly to obtain RGD-MSN/QR. Cy5 dye was modified at the 5' end of shTERT antisense strand. After sterilization, RGD-MSN/QR was incubated with shTERT for 1 h, centrifuged at 13,000 rpm to remove free RNA, precipitated and re-dispersed in DEPC water to obtain RGD-MSN/QR/shTERT.

Encapsulation efficiency and loading content of nanoparticles

The standard curve for QR concentration was constructed based on the measurement results obtained from the UV spectrophotometer. The concentration of the original sample was 0.134 mg/mL and the original dosage was 1.2 mg. Encapsulation efficiency (%) and loading content (%) of QR were calculated as follows:

$$\text{Encapsulation efficiency (\%)} = (\text{weight of drug loaded}) / (\text{weight of drug in feed}) \times 100\% = 6.7\%$$

$$\text{Loading content (\%)} = (\text{weight of drug loaded}) / (\text{weight of nanoparticles}) \times 100\% = 55.8\%$$

The concentration of shTERT before dilution was 0.06 mg/mL and the volume was 5 mL. Encapsulation efficiency (%) and loading content (%) of sh-TERT are calculated as follows:

$$\text{Encapsulation efficiency (\%)} = (\text{weight of drug loaded}) / (\text{weight of drug in feed}) \times 100\% = 3.0\%$$

$$\text{Loading content (\%)} = (\text{weight of drug loaded}) / (\text{weight of nanoparticles}) \times 100\% = 92.3\%$$

Stability of the material

The stability of the naked RNA and nano-shRNA under the action of RNase was determined. Agarose gel electrophoresis was conducted to detect the naked RNA and nano-shRNA at 0, 15, 30 min, 1, 2, and 4 h after RNA enzyme treatment. The shRNA was dissolved in chloroform, extracted and added with 0.5 M NaCl (containing 0.1% SDS) to prepare the 2% agarose gel. Electrophoresis was performed at 110 V for 15 min and then imaging was carried out under ultraviolet light.

Encapsulation efficiency of the material

The supernatant of the reaction liquid was separated and the absorption peak and Hysil ODS C18 in the 329 nm supernatant were determined by high performance liquid chromatography (HPLC), and separated with a column (4.6 × 200 mm; particle size, 5 μm).

Drug release of the material

The prepared nanoparticles was transferred into a dialysis bag (MWCO15000Da) and drug release was measured at 37 °C. Samples (500 μL) were collected at 0, 0.5, 1, 2, 4, 8, 12, and 24 h. After 48 h, the samples were stored away from light, and the corresponding volume of PBS was added. Thereafter, the release of QR was

detected through HPLC, and the released shTERT was measured using a fluorescence enzyme spectrometer (Ex.649 nm, Em.670 nm).

In vivo tumor xenograft experiment

The animal experiments were approved by the Chinese Ethics Committee of Animal Experiments (SK23035-P001-01). The care and use of laboratory animals was conducted in accordance with the US National Research Council guidelines. The 4–6-week-old male BALB/c nude mice were obtained from the Vital River Laboratory (Beijing, China) and maintained under specific pathogen free conditions at 25 °C and 50% humidity, with a 10-h:14-h light/dark cycle and free access to food and water. Totally 1×10^6 tumor cells were suspended in 100 μl PBS and injected subcutaneously into the flank of mice. Divided the mice into five groups: control group, shTERT + QR group, RGD-PEG group, RGD-MSN/QR group and RGD-MSN/QR/shTERT group. For the control group, we administered PBS via gavage. For the shTERT + QR group, we administered quercetin at a dose of 159 mg/kg via gavage, combined with 1 mg/kg of shTERT via tail vein injection. For the RGD-PEG group, we administered 100 μl of RGD-PEG via tail vein injection. For the RGD-MSN/QR group, we administered 100 μl of RGD-MSN/QR via tail vein injection. For the RGD-MSN/QR/shTERT group, we administered 100 μl of RGD-MSN/QR/shTERT via tail vein injection. We adjusted the concentrations to ensure that the total quercetin intake was consistent for the shTERT + QR group, RGD-MSN/QR group, and RGD-MSN/QR/shTERT group. After one week, the tumor size was recorded every 4 days and the tumor volume was calculated by the following equation: $\text{volume} = 0.5 \times \text{length} \times \text{width}^2$. Tumor growth was monitored until 28 days. Then, a tumor growth curve was plotted. At 28 days after cell injection, the mice were euthanized in accordance with our institute's animal ethics guidelines and animal welfare regulations. The mice were euthanized by CO₂ inhalation and the tumors were extracted. The calculation formula of tumor volume inhibition rate was as follows: $\text{tumor inhibition rate} = (\text{average volume of the control group} - \text{average volume of the experimental group}) / \text{average volume of the control group} \times 100\%$.

Histopathology and immunohistochemistry

The subcutaneous tumor tissues of nude mice were collected. Afterwards, the tumor tissue was cut into 2 μm sections from at least 3 different planes and stained with hematoxylin and eosin. Then, the histopathology was observed under a light microscope (Nikon Corporation,

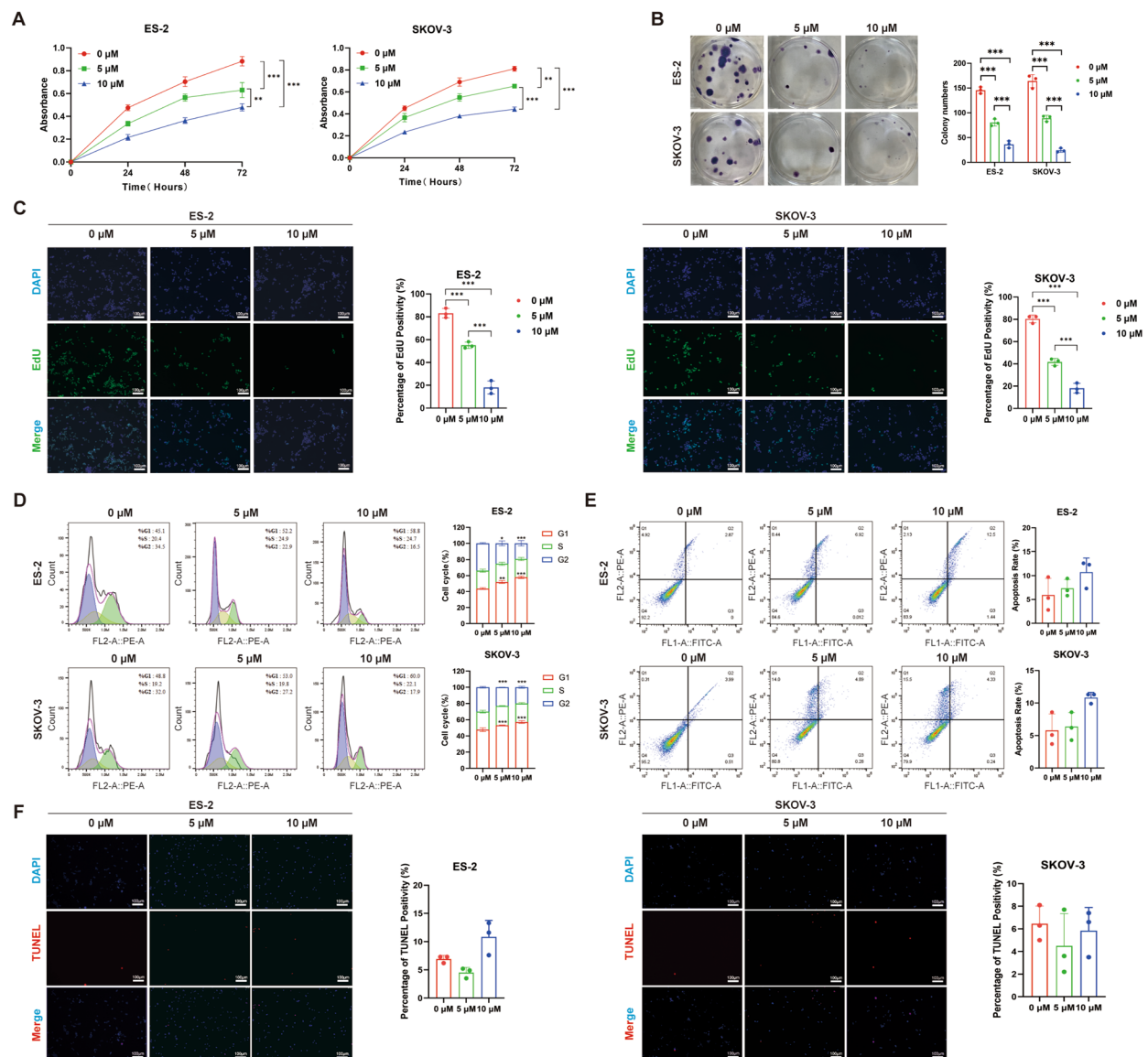


Fig. 1 Quercetin inhibits the cycle of ovarian cancer cells and unable to induce apoptosis. **A** The effect of different concentrations of quercetin on the proliferation level of ovarian cancer cells was measured by CCK-8; **B** The effect of different concentrations of quercetin on the proliferation level of ovarian cancer cells was tested by cell clone formation assay; **C** The effect of different concentrations of quercetin on ovarian cancer cell proliferation was tested by EDU assay; **D** The effect of different concentrations of quercetin on the ovarian cancer cell cycle was measured by flow cytometry; **E** The effect of various concentrations of quercetin on apoptosis of ovarian cancer cells was determined by flow cytometry; **F** The effect of different concentrations of quercetin on apoptosis in ovarian cancer cells was examined by the TUNEL assay. * $p < 0.05$, *** $p < 0.001$

Japan). The paraffin-embedded sections were dehydrated and stained with immunoperoxidase. Afterwards, antigen epitope was exposed with 10 mM citrate buffer through microwave treatment. Subsequently, the sections were incubated with rabbit polyclonal antibodies. Primary antibody staining was detected with the peroxidase-coupled anti-rabbit IgG. Images were obtained under the

Leica DM4000B fluorescence microscope equipped with a digital camera. The semi-quantitative scoring method was used for the quantitative analysis of immunohistochemistry. The staining intensity was typically classified as no stain (0 points), weak stain (1 point), moderate stain (2 points), and strong stain (3 points); the proportion of positive cells was graded based on the percentage

of positive cells out of the total number of cells, such as 0% -5% for 0 points, 5% -25% for 1 point, 25% -50% for 2 points, 50% -75% for 3 points, and over 75% for 4 points. The final semi-quantitative score was obtained by multiplying the staining intensity score by the positive cell ratio score.

Statistical analysis

All data were obtained from three independent experiments and expressed as mean \pm standard deviation. Differences between two groups were analyzed using paired or unpaired t-tests. Single-factor analysis of variance (ANOVA) and Tukey tests were adopted to assess differences among multiple groups. Pearson correlation coefficients were calculated to examine the correlation of different gene expression levels. A p-value of $^*p < 0.05$, $^{**}p < 0.01$ and $^{***}p < 0.001$ was considered statistically significant.

Results

Quercetin inhibits the cell cycle of ovarian cancer but does not induce apoptosis

Quercetin showed good tumor inhibiting effect in many types of tumors. To investigate whether quercetin could induce the apoptosis of OC, we applied quercetin at different concentrations to interfere with OC cell lines ES-2 and SKOV-3, so as to detect the effect of quercetin on OC. Changes in the proliferative ability of OC cell lines were detected by CCK-8 assay after intervention with different concentrations of quercetin. The results of CCK-8 assay suggested that quercetin at 5 μ M and 10 μ M inhibited the proliferation of OC (72 h: 0 μ M vs. 5 μ M, ES-2: $p = 0.0004$, SKOV-3: $p = 0.0008$; 0 μ M vs. 10 μ M, ES-2: $p = 0.0003$, SKOV-3: $p = 0.0002$), and the inhibitory effect was more obvious with the increase in concentration and the extension of time (Fig. 1A). The above views were verified by cell cloning assay and EdU assay (cell cloning assay: 0 μ M vs. 5 μ M, ES-2: $p = 0.0003$, SKOV-3: $p = 0.0004$; 0 μ M vs. 10 μ M, ES-2: $p = 0.0001$, SKOV-3: $p = 0.0001$; EdU assay: 0 μ M vs. 5 μ M, ES-2: $p = 0.0004$, SKOV-3: $p = 0.0003$; 0 μ M vs. 10 μ M, ES-2: $p = 0.0003$, SKOV-3: $p = 0.0002$) (Fig. 1B, C). It has been evidenced that quercetin can block cell cycle in cancers like liver cancer, breast cancer, and lung cancer. In this study, flow cytometry was conducted to detect the changes in cell cycle of OC after intervention with different concentrations of quercetin. It was discovered that after quercetin intervention, OC cells accumulated at the G0/G1 phase, and the degree increased with the increase in quercetin concentration (0 μ M vs. 5 μ M, ES-2: $p = 0.0006$, SKOV-3: $p = 0.0008$; 0 μ M vs. 10 μ M, ES-2: $p = 0.0005$, SKOV-3: $p = 0.0004$) (Fig. 1D).

We further explored whether quercetin could induce the apoptosis of OC cells. The apoptosis level of OC cell lines after different concentrations of quercetin was detected by flow cytometry. As a result, the apoptosis level of OC was not significantly affected by quercetin (0 μ M vs. 5 μ M, ES-2: $p = 0.7366$, SKOV-3: $p = 0.2478$; 0 μ M vs. 10 μ M, ES-2: $p = 0.4852$, SKOV-3: $p = 0.8263$) (Fig. 1E). The TUNEL assay also confirmed the results of flow cytometry (0 μ M vs. 5 μ M, ES-2: $p = 0.3646$, SKOV-3: $p = 0.9624$; 0 μ M vs. 10 μ M, ES-2: $p = 0.5468$, SKOV-3: $p = 0.3663$) (Fig. 1F). Therefore, quercetin can only inhibit the proliferation of OC cells but not induce the apoptosis of OC cells.

Quercetin inhibits the proliferation of OC cells via the P53 pathway, as explored based on network pharmacology

To explore the specific mechanism by which quercetin inhibited the proliferation of OC cells but failed to induce apoptosis, we conducted a network pharmacology analysis. A total of 507 drug target genes were obtained by screening the quercetin active ingredients from the TCMSP database. With "ovarian cancer" being the keyword, 13,078 OC-related genes were identified based on the GeneCard disease gene database. The targets of quercetin active ingredients were intersected with those associated with OC disease, and altogether 484 candidate action genes were obtained (Fig. 2A). The selected action genes were imported into the STRING database for PPI analysis. Cytoscape software was employed to construct the interaction network diagram (Fig. 2B), in which TP53 had the highest interaction score. Moreover, GO and KEGG enrichment analyses were performed on the action genes, and it was found that these genes were enriched into pathways like "KEGG: Pathways in cancer", and "KEGG: p53 signaling pathway" (Fig. 2C, D).

Previous studies have reported that the activation of P53 can inhibit the cell cycle and proliferation by activating P21/Rb [18]. Meanwhile, the activation of P53 can also up-regulate BAX and induce apoptosis (Fig. 2E) [19]. Based on the correspondence between the active ingredients and the potential targets, the core target proteins were subjected to molecular docking with quercetin. As a result, quercetin had a stable binding with P53 and P21 (Fig. 2F–G). Western blotting was performed to verify the expression levels of the above key proteins, and it was found that after quercetin intervention, the expression levels of P53, BAX and Bcl-2 were not significantly changed, while that of P21 was significantly up-regulated with the increase in quercetin (0 μ M vs. 5 μ M, ES-2: $p = 0.0036$, SKOV-3: $p = 0.3949$; 0 μ M vs. 10 μ M ES-2: $p = 0.0004$, SKOV-3: $p = 0.0007$) (Fig. 2H). Therefore, in OC cells, the inability of quercetin to activate P53 is the cause for its failure to induce apoptosis.

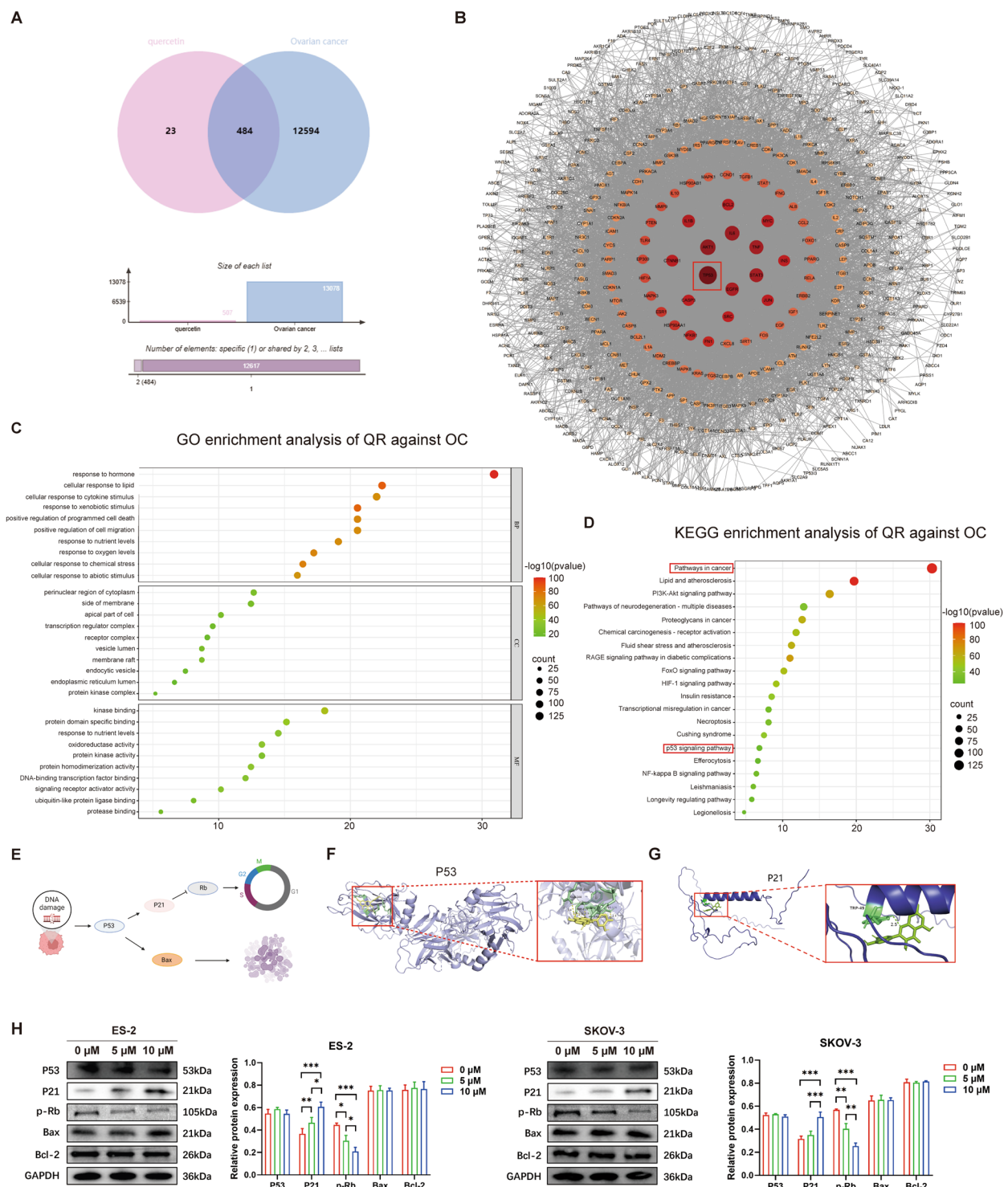


Fig. 2 Quercetin inhibits ovarian cancer via the P53 pathway by network pharmacological analysis. **A** Venn diagram of targets of active components in quercetin and associated targets in ovarian cancer; **B** PPI networks of the intersection genes; **C** KEGG enrichment analysis of intersection genes; **D** GO enrichment analysis of intersection genes; **E** P53 pathway suppresses the cell cycle and induces apoptosis; **F** Molecular docking of quercetin to P53; **G** Molecular docking of quercetin to P21; **H** Expression level of P53 pathway protein after different concentrations of quercetin intervention by Western Blot in ovarian cancer cells. * $p < 0.05$, ** $p < 0.01$, *** $p < 0.001$

Based on proteomics and bioinformatics analyses, TERT excessively binds to P53 in OC, making quercetin unable to activate P53

To explore the potential mechanism of quercetin in inhibiting OC, we constructed the subcutaneous tumorigenic nude mouse models with ES-2 and SKOV-3 OC cell lines, and divided them into the control group and the quercetin group for gavage of normal saline and quercetin, respectively. The sample size of each group was three ($n=3$). The animals were killed 28 days later (Fig. 3A), and the tumors were dissected (Fig. 3B). Through comparing the tumor size, we found that the tumor size in the quercetin group was slightly smaller than that in the control group, but the difference was not significant (control vs. quercetin groups ES-2: $p=0.0786$ SKOV-3: $p=0.0432$) (Fig. 3C, D). The mouse tumors constructed with two cell lines were subjected to proteomic analysis. In the proteomics analysis of the ES-2 subcutaneous tumorigenic model mice, altogether 106 differential genes were detected upon the screening conditions of $|\log \text{fold-change}| > 1$ and $p \text{ value} < 0.05$. Compared with the control group, there were 48 up-regulated and 58 down-regulated genes in the quercetin group (Fig. 3E&G). Under the same screening conditions, a total of 470 differential genes were identified in the SKOV-3 subcutaneous tumorigenic model mice. Relative to the control group, 205 up-regulated and 265 down-regulated genes were detected in the quercetin group (Fig. 3F&H). The differential genes obtained by the two proteomics analyses were intersected, which revealed 4 common up-regulated (Fig. 3I) and 5 common down-regulated genes (Fig. 3J). We subsequently performed KEGG and GO enrichment analyses on the two groups of differential genes respectively (Fig. 3K–N), and the results indicated that the two groups of differential genes were enriched to the “KEGG: P53 signaling pathway”. Therefore, this further confirms that in OC, quercetin can affect the P53 pathway.

However, the above results still did not explain why quercetin failed to activate P53. To further explore the reason, we used the TCGA-OC database for the correlation analysis between TP53 and other genes (Fig. 3O–P), and discovered that TERT was significantly positively correlated with TP53. TERT, a telomerase reverse transcriptase, plays a key role in the formation of cancer and is highly expressed in OC as a potential therapeutic target for OC [20]. The Uniprot database was employed to predict the interaction between P53 and TERT proteins (Fig. 3Q), and CO-IP assays were carried out on P53 and TERT proteins in OC cell lines (Fig. 3R). The results indicated that there was an interaction between P53 and TERT. This suggests that the inability of quercetin to activate P53 protein in OC may be related to TERT binding to P53, which limited the role of P53 in inducing cell apoptosis.

Quercetin induces the apoptosis of OC cells after TERT knockdown by activating P53/BAX

To verify this hypothesis, we performed TERT knockdown on OC cells (Fig. 4A). The effect of shTERT combined with quercetin on the changes in OC cell proliferation was detected by CCK-8 assay. The results suggested that the combination of shTERT with quercetin better inhibited the proliferation of OC (Control vs. QR+shTERT, ES-2: $p=0.0008$, SKOV-3: $p=0.0006$; QR vs. QR+shTERT, ES-2: $p=0.0427$, SKOV-3: $p=0.0097$; shTERT vs. QR+shTERT, ES-2: $p=0.0378$, SKOV-3: $p=0.0154$) (Fig. 4B). Flow cytometry showed that OC cells accumulated at the G1 and S phases after combined intervention, thus better inhibiting cell cycle (Control vs. QR+shTERT, ES-2: $p=0.0004$, SKOV-3: $p=0.0002$; QR vs. QR+shTERT, ES-2: $p=0.0372$, SKOV-3: $p=0.0673$; shTERT vs. QR+shTERT, ES-2: $p=0.0078$, SKOV-3: $p=0.0063$).

We detected the apoptosis of OC cell lines after intervention with different concentrations of quercetin by

(See figure on next page.)

Fig. 3 Quercetin unable to induce apoptosis in ovarian cancer was analyzed by proteomics and TCGA database. (A) Quercetin non-intervention/intervention of mice and tumor xenografts in the CDX model constructed by ES-2; (B) Quercetin non-intervention/intervention of mice and tumor xenografts in the CDX model constructed by SKOV-3; (C) The effect of non-intervention/intervention of quercetin on tumor volume in the CDX model constructed by ES-2; (D) The effect of non-intervention/intervention of quercetin on tumor volume in the CDX model constructed by SKOV-3; (E) Histogram of differential proteins without intervention/intervention of quercetin in the CDX model constructed by ES-2; (F) Histogram of differential proteins without intervention/intervention of quercetin in the CDX model constructed by SKOV-3; (G) Volcanic map of differential proteins without intervention/intervention of quercetin in the CDX model constructed by ES-2; (H) Volcanic map of differential proteins without intervention/intervention of quercetin in the CDX model constructed by SKOV-3; (I) Wayn diagram of upregulated differential proteins in the CDX model constructed by ES-2 and SKOV-3; (J) Wayn diagram of downregulated differential proteins in the CDX model constructed by ES-2 and SKOV-3; (K) KEGG enrichment analysis of differential proteins in the CDX model constructed by ES-2; (L) GO enrichment analysis of differential proteins in the CDX model constructed by ES-2; (M) KEGG enrichment analysis of differential proteins in the CDX model constructed by SKOV-3; (N) GO enrichment analysis of differential proteins in the CDX model constructed by SKOV-3; (O) Heatmap of the visualized coexpression of TP53 with other genes from the TCGA database; (P) TP53 and TERT expression correlation analysis from the TCGA database; (Q) Protein molecular docking of P53 and TERT; (R) CO-IP experiments detect P53 and TERT binding

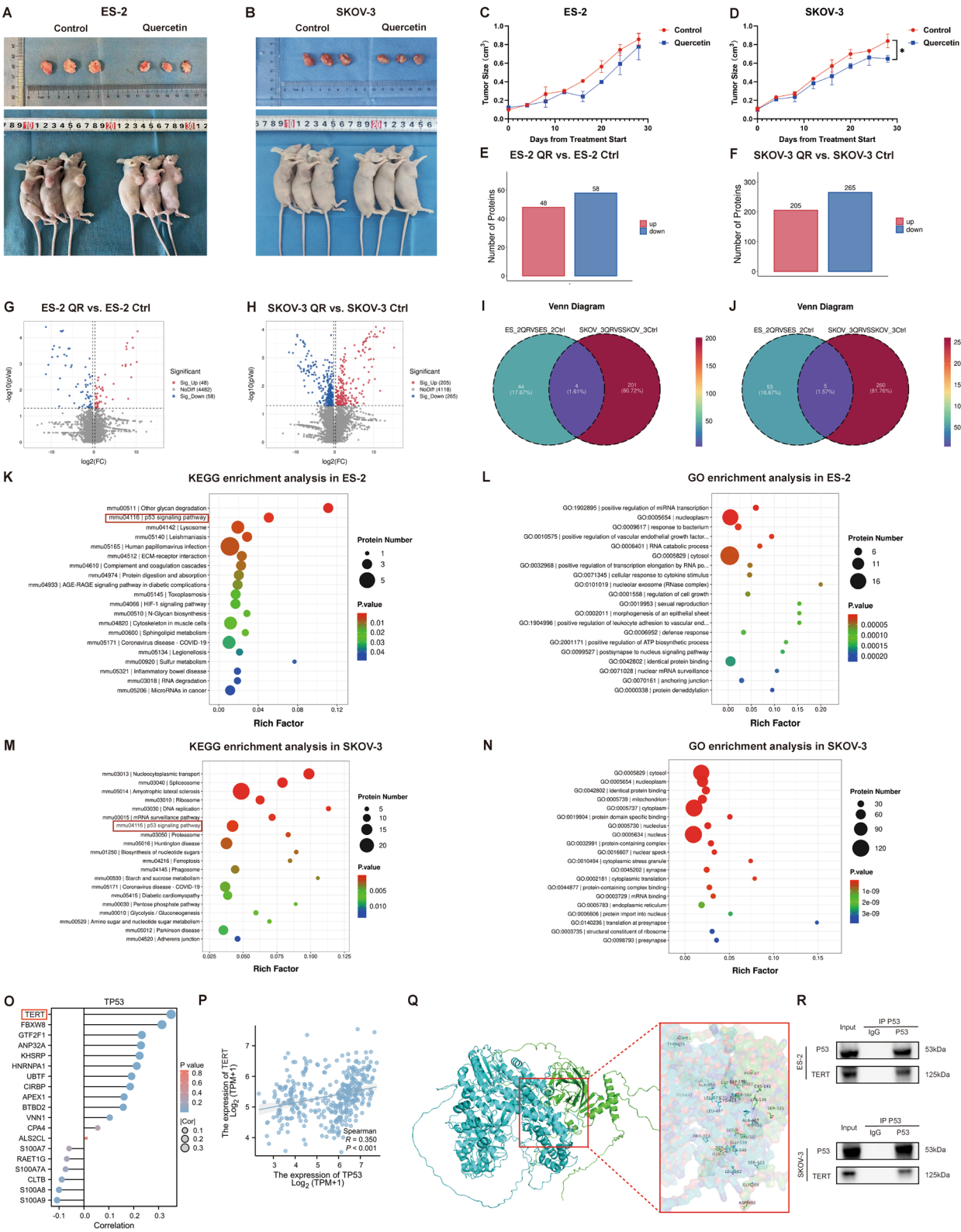


Fig. 3 (See legend on previous page.)

flow cytometry. The results suggested that the apoptosis level of OC cells was significantly enhanced after the combined intervention of shTERT with quercetin (Control vs. QR+shTERT, ES-2: $p=0.0007$, SKOV-3: $p=0.0006$; QR vs. QR+shTERT, ES-2: $p=0.0002$, SKOV-3: $p=0.0003$; shTERT vs. QR+shTERT, ES-2: $p=0.0007$, SKOV-3: $p=0.0006$) (Fig. 4D). Western blotting assay was performed to verify the expression levels of the above key proteins, and it was found that after the combined intervention, the expression levels of P53 (Control vs. QR+shTERT, ES-2: $p=0.0004$, SKOV-3: $p=0.0002$; QR vs. QR+shTERT, ES-2: $p=0.0006$, SKOV-3: $p=0.0003$; shTERT vs. QR+shTERT ES-2: $p=0.0026$, SKOV-3: $p=0.0032$) and BAX (Control vs. QR+shTERT, ES-2: $p=0.0001$, SKOV-3: $p=0.0002$; QR vs. QR+shTERT, ES-2: $p=0.0005$, SKOV-3: $p=0.0004$; shTERT vs. QR+shTERT ES-2: $p=0.0009$, SKOV-3: $p=0.0006$) were significantly up-regulated, while that of Bcl-2 significantly decreased (Control vs. QR+shTERT, ES-2: $p=0.0003$, SKOV-3: $p=0.0004$; QR vs. QR+shTERT, ES-2: $p=0.0005$, SKOV-3: $p=0.0007$; shTERT vs. QR+shTERT ES-2: $p=0.0001$, SKOV-3: $p=0.0002$) (Fig. 4E). The combined intervention of quercetin with shTERT could better inhibit the proliferation of OC and induce apoptosis. Meanwhile, such results also further verify that the inability of quercetin to activate P53 protein is related to TERT binding to p53.

Preparation and characterizations of RGD-MSN/QR/shTERT

Our in vitro experiments demonstrated the advantages of the combined intervention of quercetin with shTERT in inducing OC apoptosis. However, being prone to degradation of shTERT in body, low bioavailability of quercetin and lack targeting of combination therapy are still problems to be solved for in vivo therapy. To achieve the co-delivery of quercetin and shTERT and solve the above problems, we prepared the QR-loaded mesoporous silica nanoparticles (Fig. 5A). Firstly, the MSN/QR drug-loaded nanoparticles loaded with the TCM monomer QR were synthesized; secondly, drug-loaded nanoparticles were coated with positively charged RGD-PEG, so that the nanoparticles could target drugs, and the synthesized drug-carrying nanoparticles were positively charged.

Finally, shTERT was adsorbed by static electricity to form RGD-MSN/QR/shTERT.

Next, we employed a variety of technical methods to characterize the nanoparticles. Through performing dynamic light scattering measurements, it was found that the hydrodynamic diameter was 239.53 nm, while the diameter of the nanoparticles increased to 242.61 nm (Fig. 5B), and the zeta potential changed from 28.74 ± 3.74 mV to 9.14 ± 1.35 mV when shTERT was connected (Fig. 5C). The particle size distribution of both nanoparticles was relatively narrow, indicating that the synthesized nanoparticles maintained good uniformity. Transmission electron microscopy (TEM) images showed that both RGD-MSN/QR and RGD-MSN/QR/shTERT had uniform spherical structures (Fig. 5D).

We further tested the drug release levels of RGD-MSN/QR and RGD-MSN/QR/shTERT (Fig. 5E), and discovered that the release rates of QR and shTERT were relatively fast at the initial stage, and gradually became flattened after 12 h. Since shRNA is linked with the disadvantages of poor stability and easy degradation of ribonuclease (RNase), we adopted nanoparticles encapsulation to solve this dilemma while improving the efficiency of drug delivery. To verify the protective effect of nanoparticles on shTERT, the naked shRNA and RGD-MSN/QR/shTERT were incubated with RNase for different time periods (0 min, 15 min, 30 min, 1 h, 2 h, 4 h, 8 h, 12 h), and then agar-gel electrophoresis was performed. We observed the rapid degradation of naked siRNA in the presence of RNase, while the nanoparticles maintained the major structural integrity of shRNA after 12 h (Fig. 5F). The above results show that the nanoparticles have high stability and can protect the degradation of shRNA, which lay a good foundation for the follow-up in vivo experiments.

Furthermore, to verify the uptake of nanoparticles by OC cells in vitro, shTERT was labeled with Cy5, and OC cells were intervened with PBS, shTERT, and RGD-MSN/QR/shTERT, respectively. Later, cell uptake was studied through confocal laser microscopy. The images revealed that, incubation with RGD-MSN/QR/shTERT exhibited the strongest intracellular fluorescence intensity, while cells treated with shTERT had slightly weaker fluorescence intensity and cells cultured with PBS showed no fluorescence (Fig. 5G). This suggests that the

(See figure on next page.)

Fig. 4 Quercetin combine with shTERT induced apoptosis in ovarian cancer in vitro. **(A)** TERT knockdown of the ovarian cancer cell lines ES-2 and SKOV-3; **(B)** The effect of quercetin combine with shTERT on the proliferation level of ovarian cancer cells was measured by CCK-8; **(C)** The effect of quercetin combine with shTERT on the ovarian cancer cell cycle was measured by flow cytometry; **(D)** The effect of quercetin combine with shTERT on apoptosis of ovarian cancer cells was determined by flow cytometry; **(E)** Expression level of P53 pathway protein after quercetin combine with shTERT intervention by Western Blot in ovarian cancer cells. * $p < 0.05$, ** $p < 0.01$, *** $p < 0.001$

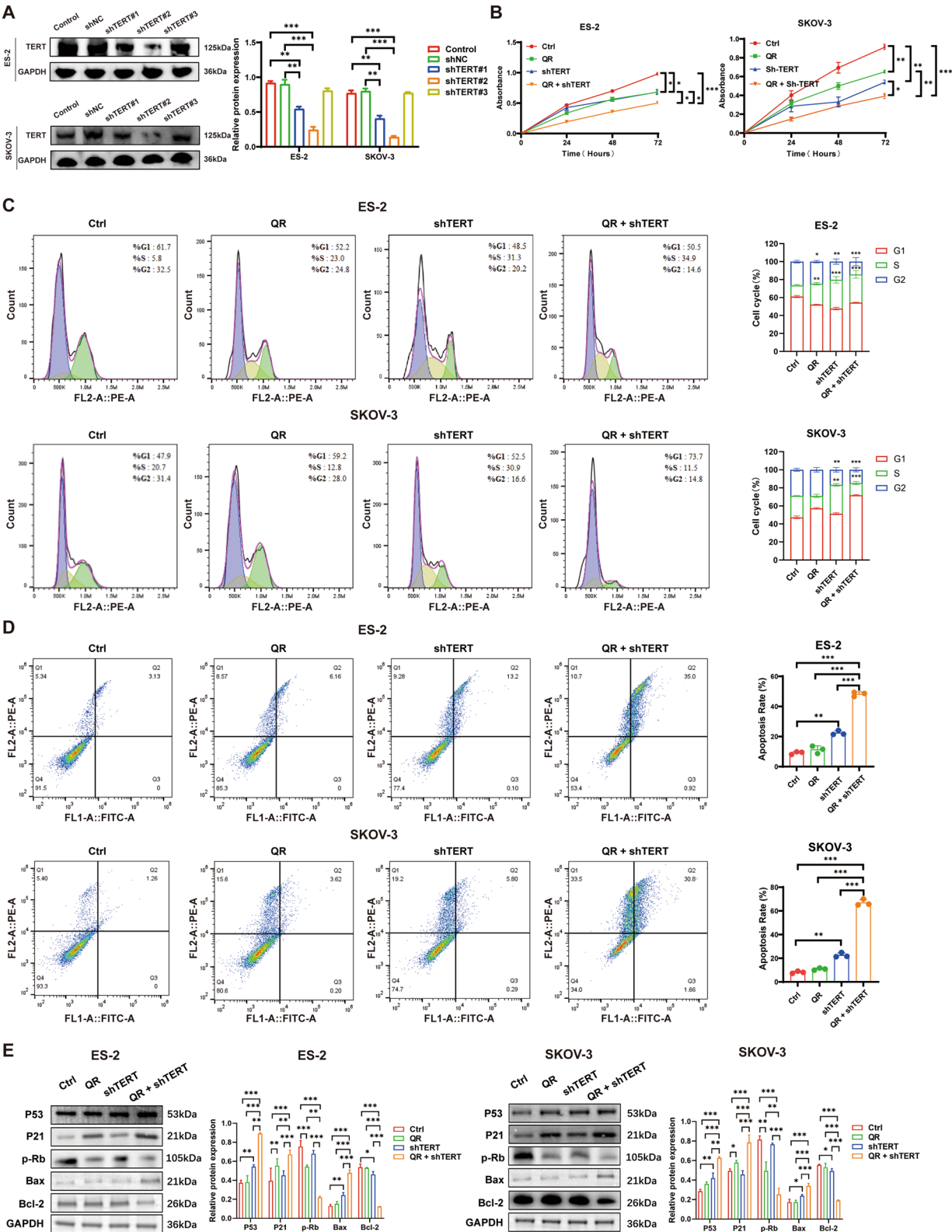


Fig. 4 (See legend on previous page.)

nanoparticles can be taken up by OC cells. At the same time, to explore the targeting of nanoparticles, PBS, shTERT and RGD-MSN/QR/shTERT were injected intravenous into the tail vein of tumorigenic mice (Fig. 5H), and the results demonstrated that only the RGD-MSN/QR/shTERT group showed strong fluorescence at the tumor site, suggesting that the nanoparticles have good targeting property.

Finally, we evaluated the safety of nanoparticles by injecting PBS, RGD-PEG, RGD-MSN/QR, and RGD-MSN/QR/shTERT into the tail vein of mice, respectively. After nanoparticle intervention, mice did not show hemolysis (Fig. S1A). By comparing the H&E stained sections of the heart, liver, spleen, lung, kidney and intestinal tissues, it was discovered that there was no difference between the nanoparticle group and the control group (Fig. S1B). Serum biochemical analyses (serum alanine aminotransferase (ALT), aspartate aminotransferase (AST), alkaline phosphatase (ALP), total bilirubin (TBIL) and urea nitrogen (BUN)) and blood routine detection were performed [white blood cell (WBC), red blood cell (RBC), and platelet (PLT)] to evaluate the biosafety of nanoparticles in vivo. The blood cell and serum biochemical indexes of all mice were within the normal range, and the differences were negligible (Fig. S1C-J), further proving that the nanoparticles have certain safety.

The in vivo anti-OC effect of RGD-MSN/QR/shTERT

To further verify the anti-OC effect of RGD-MSN/QR/shTERT in vivo, subcutaneous tumorigenic mice were divided into the control group, shTERT+QR group, RGD-PEG group, RGD-MSN/QR group, and RGD-MSN/QR/shTERT group, and injected with PBS, shTERT, RGD-PEG, RGD-MSN/QR and RGD-MSN/QR/shTERT, and intervened respectively (Fig. 6A). The sample size of each group was three ($n=3$). After 28 days of intervention, the mice were killed (Fig. 6B), and the tumors were dissected (Fig. 6C). We found that the tumors of mice in the RGD-MSN/QR/shTERT group were significantly smaller than those in the control group and shTERT+QR group (Control vs. RGD-MSN/QR/shTERT, ES-2: $p=0.0007$, SKOV-3: $p=0.0004$; RGD-MSN/QR vs. RGD-MSN/QR/shTERT, ES-2: $p=0.0092$,

SKOV-3: $p=0.0003$; shTERT+QR vs. RGD-MSN/QR/shTERT, ES-2: $p=0.0326$, SKOV-3: $p=0.0084$) (Fig. 6D).

Meanwhile, the expression levels of key proteins in five groups of mice were detected by immunohistochemistry. As a result, the expression levels of P53 and BAX in RGD-MSN/QR/shTERT group were significantly higher than those in the other four groups, and the expression level of Bcl-2 was significantly lower than those in the other four groups. Meanwhile, we also found that the expression levels of P21 in the RGD-MSN/QR and RGD-MSN/QR/shTERT groups were significantly higher than those in the other three groups, and that of p-Rb was significantly lower than those in the other three groups (Fig. 6E). This further proves that quercetin combined with shTERT can activate the P53/BAX signaling pathway, and our constructed RGD-MSN/QR/shTERT can safely and effectively exert the combined anti-OC effect in vivo.

Discussion

The treatment of OC is encountered with numerous difficult problems at present. First, OC is prone to widespread metastasis, which greatly increases the difficulty and complexity of treatment [21]. Secondly, for advanced patients, chemotherapy is the only proven effective strategy currently, but with the progress of treatment, cancer cells often develop drug resistance, and may also induce a series of serious adverse reactions, seriously affecting the quality of life of patients and the tolerance of subsequent treatment [2]. Moreover, OC has a high recurrence rate; for the treatment of recurrent OC, the effective treatment options are relatively limited, the choice of drugs is more difficult, and the disease progression is often faster, accompanied by the worse prognosis [3]. Therefore, there is an urgent need to study and innovate a safe and effective treatment to improve the prognosis and quality of life of OC patients.

In this study, we first used quercetin, a natural compound with good therapeutic effect on tumors, to intervene with OC cells, and found that it only inhibited the cell proliferation, but not induced cell apoptosis. Additionally, upon network pharmacology and proteomics analyses, the excessive TERT binding to P53 in OC was

(See figure on next page.)

Fig. 5 Preparation and characterization of RGD-MSN/QR/shTERT. (A) Schematic diagram of RGD-MSN/QR/shTERT synthesis; (B) Hydrodynamic size distribution of RGD-MSN, RGD-MSN/QR and RGD-MSN/QR/shTERT by DLS; (C) Zeta potential of RGD-MSN, RGD-MSN/QR and RGD-MSN/QR/shTERT; (D) TEM images of RGD-MSN, RGD-MSN/QR and RGD-MSN/QR/shTERT; (E) The release kinetics of QR and shTERT from RGD-MSN/QR and RGD-MSN/QR/shTERT at pH 7.4 and 37 °C; (F) Stability of naked shTERT and RGD-MSN/QR/shTERT against RNase measured by agarose gel electrophoresis; (G) CLSM images of ES-2 and SKOV-3 cells incubated with PBS, Free Cy5-shTERT and RGD-MSN/QR/shTERT for 4 h. Scale bar: 50 μ m; (H) The bioluminescence images of tumour-bearing mice 12 h after injection of PBS, naked Cy5-shTERT and RGD-MSN/QR/shTERT to observe their targeting ovarian cancer ability

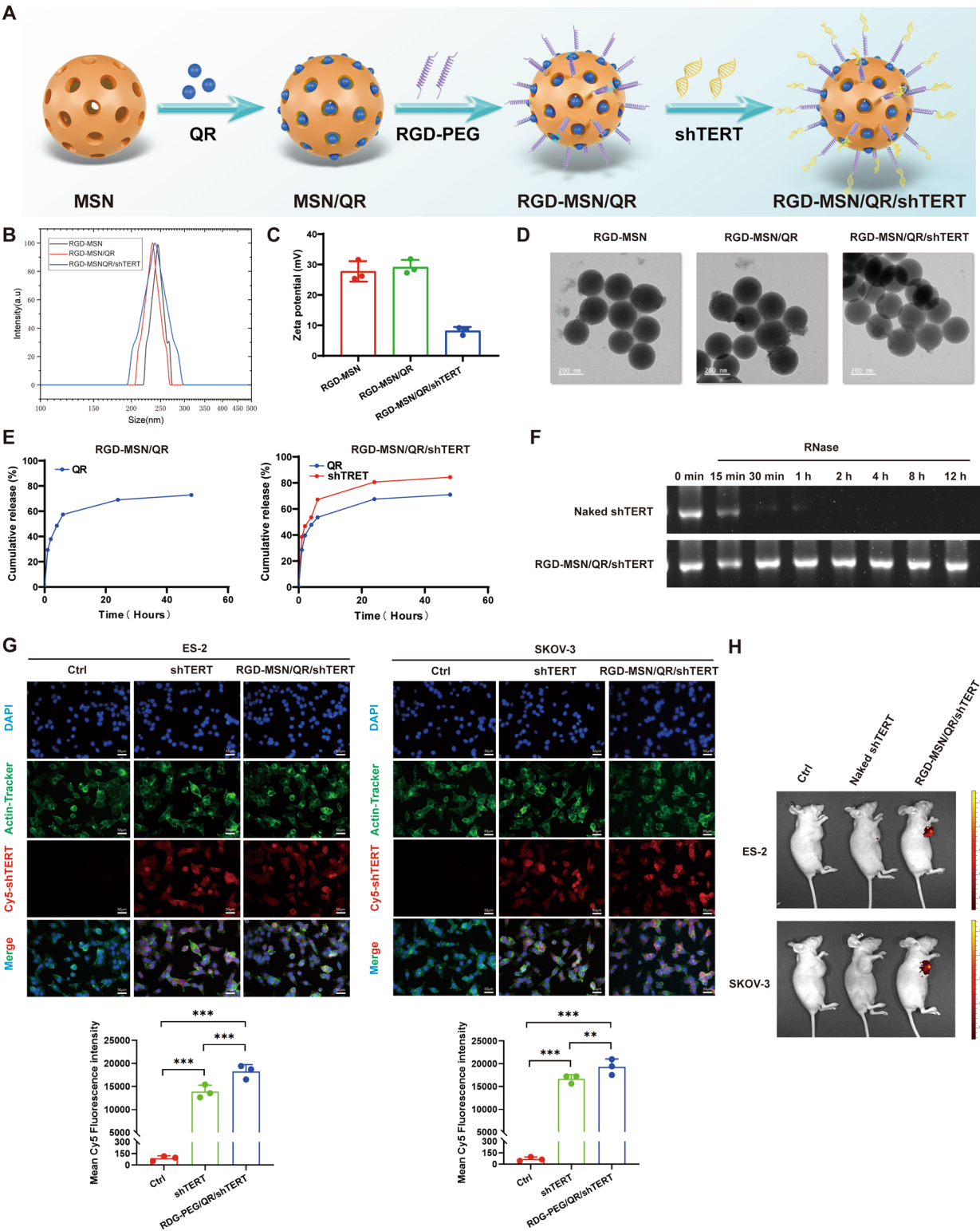


Fig. 5 (See legend on previous page.)

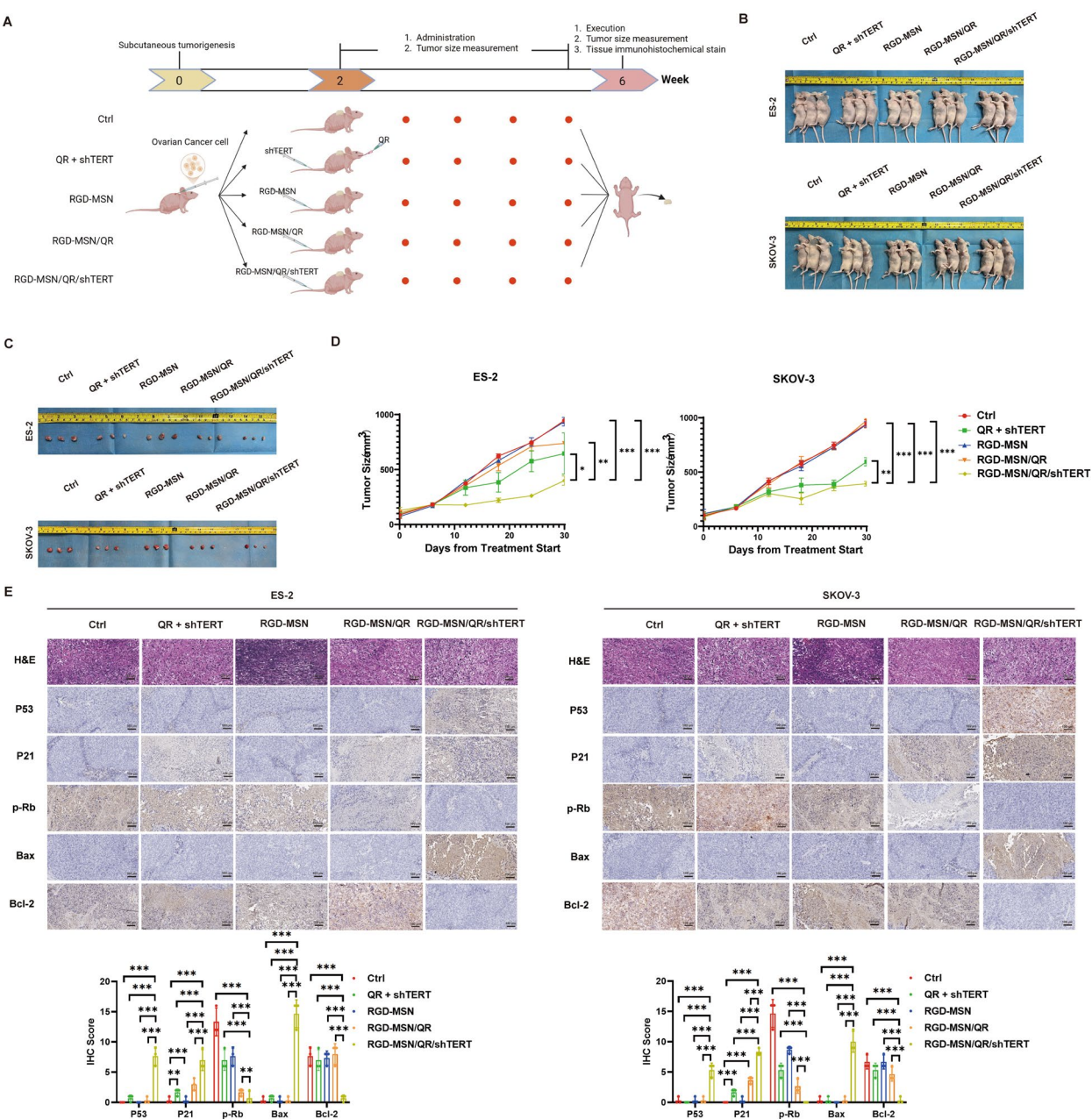


Fig. 6 The effect of RGD-MSN/QR/shTERT against inhibition in ovarian cancer in vivo. **(A)** The intervention flow chart, n = 5; **(B, C & D)** The effect of PBS, Quercetin combine with shTERT, RGD-MSN, RGD-MSN/QR and RGD-MSN/QR/shTERT on tumor size in tumour-bearing mice; **(E)** The effect of PBS, Quercetin combine with shTERT, RGD-MSN, RGD-MSN/QR and RGD-MSN/QR/shTERT on the expression level of P53 pathway protein by immunohistochemical stain in tumour-bearing mice. * $p < 0.05$, ** $p < 0.01$, *** $p < 0.001$

identified as the cause of this phenomenon. Secondly, we used shTERT combined with quercetin for in vitro intervention and discovered that the combined treatment better inhibited the proliferation of OC while inducing apoptosis. Finally, to make this combined treatment safe, effective and targeted in vivo, we designed and prepared a new nanoparticle (RGD-MSN/QR/shTERT) for the

combined administration of quercetin and shTERT. As revealed by in vivo experiments, RGD-MSN/QR/shTERT showed favorable targeting ability, remarkable OC inhibiting effect and negligible adverse reactions.

Quercetin has demonstrated a variety of anti-tumor mechanisms, providing a new potential approach for tumor treatment, but further research is still needed to

fully explore its clinical application value. Firstly, quercetin has a significant effect on inducing apoptosis. According to numerous studies, it can trigger the apoptosis of cancer cells via a variety of pathways. In breast cancer studies, quercetin can reduce the expression level of NADH reductase coenzyme I in breast cancer cells, thus promoting the apoptosis of cancer cells [22]. In pancreatic cancer research, quercetin can reduce the expression level of FLICE-like inhibitory protein in cells, enhance the sensitivity of cancer cells to TRAIL-induced apoptosis, and thus induce the apoptosis of pancreatic cancer cells [23]. This ability to induce apoptosis of different cancer cells reflects the key role of quercetin in tumor treatment. Secondly, the regulation of quercetin on cell cycle is also an important mechanism of its anti-tumor activity. In the study on colon cancer, quercetin can inhibit the vitality of colon cancer cells and induce their apoptosis through MAPKs pathway, while arresting the cell cycle at a specific stage and effectively preventing the proliferation of cancer cells [24]. In the research on lung cancer, quercetin can reduce the phosphorylation of histone proteins, thus leading to the arrest of cancer cell cycle and inhibiting tumor growth [25]. It shows great potential in anti-tumor treatment [26]. However, in our study, due to the over-binding of P53 to TERT in OC, quercetin only inhibited OC proliferation and cell cycle, but did not induce apoptosis, which greatly limits the application of quercetin in the treatment of OC.

In the complex network of cell cycle regulation, the P53/P21 pathway occupies a key position and plays an important and fine regulatory role in the process of cell cycle. Under normal circumstances, P53 protein, as the “guardian of the genome”, always monitors the stability of the intracellular environment. Once the cells experience stress signals such as DNA damage, oncogene activation, hypoxia or telomere shortening, P53 protein will be activated and accumulated rapidly. After its activation, it can bind specifically to the promoter region of P21 gene to drive the transcriptional expression of P21 gene [27]. As a potent inhibitor of cyclin-dependent kinase (CDK), P21 binds tightly to the CDK-cyclin complex to inhibit its kinase activity. Complexes such as CDK4/6-cyclin D and CDK2-cyclin E play a key role in the transition from G1 phase to S phase of the cell cycle. The binding of P21 to these complexes effectively blocks the phosphorylation modification of retinoblastoma protein (Rb), thereby maintaining the stability of the genome [28]. In certain types of tumors, the P53 gene is often mutated or missing, resulting in the loss or abnormality of P53 protein function, as well as the inability to effectively activate the expression of P21. As a result, the expression level of P21 is significantly down-regulated, the cell cycle is out of control, and

the cell proliferation rate is greatly improved. Apart from the classical P53 direct regulation of P21 pathway, there are other signaling pathways interweaving with the P53/P21 pathway to synergistically induce tumors, such as the P53/BAX pathway. The P53/BAX pathway has a key role in inducing tumor cell apoptosis and has far-reaching significance for the development of cancer treatment strategies. When cells suffer from DNA damage caused by carcinogenic factors, P53 protein rapidly accumulates and binds to the BAX gene promoter region, enhancing its transcriptional activity and promoting the increase in BAX protein level, ultimately leading to the execution of the apoptosis procedure [29]. In OC cells, quercetin bound to P21 to inhibit cell proliferation. However, the over-binding of TERT to P53 not only restricted P53-mediated apoptosis but also blocked quercetin's interaction with P53. When TERT was silenced using shTERT, P53 was liberated to induce apoptosis and strengthen cell cycle arrest. Concurrently, quercetin gained access to P53, intensifying both apoptosis and cell cycle arrest (Sch. 1). We hypothesize that quercetin enhances the stability of P53 protein, protecting it from degradation and thereby potentiating its apoptotic and cell cycle-regulatory effects, but this needs to be further confirmed.

TERT is telomerase reverse transcriptase, which is involved in the repair of telomeres and plays a crucial role in the process of OC cell cycle. From the perspective of telomere maintenance, TERT, as a key catalytic subunit of telomerase, stabilizes the terminal structure of chromosomes by extending the telomere length, thereby preventing replicative senescence or apoptosis of cells caused by telomere shortening, and continuously carrying out the cell cycle, enabling the continuous proliferation of tumor cells and the development of tumor [30]. The role of TERT also varies at different stages of the cell cycle. During the transition from G1 phase to S phase, TERT promotes cells to successfully pass the restriction point and enter the DNA synthesis phase by regulating the activities of related cyclin and CDK. In the S phase, the function of TERT to maintain telomere length is essential to ensure the integrity of DNA replication, preventing DNA damage and cell cycle arrest due to telomere abnormalities [31]. In our study, after the combined intervention, OC cells not only accumulated at the G0/G1 phase, but also more accumulated at the S phase, so as to better inhibit the cell cycle. This process may be associated with the silencing of TERT, and the combined treatment can not only induce apoptosis, but also better block the cell cycle.

In the process of combined application of quercetin with shTERT in vivo against OC, we need to solve many

problems such as low availability, poor drug targeting and poor drug synergy of the natural compound quercetin. Because of its unique structure and characteristics, MSN has been used in the research of tumor treatment as a highly safe, controllable drug delivery carrier. Using MSN as a carrier, numerous natural compounds overcome the defects of poor water solubility, greatly improving the bioavailability [32]. Meanwhile, MSN has two functional surfaces, which can be easily functionalized [33] and properly connected or modified with other materials. On the one hand, it is assembled with polycations, so that its surface is positively charged, and it can be attached to shRNA, facilitating the synergistic administration with natural compounds. On the other hand, it can also bind to some targeted functional peptides, so that the drug can better target the tumor.

Conclusion

In summary, this study demonstrates the mechanism and therapeutic advantages of the combination of quercetin with shTERT against OC. Based on this mechanism, a novel nanoparticle (RGD-MSN/QR/shTERT) was designed and prepared for the combined administration of quercetin with shTERT in vivo. The results showed RGD-MSN/QR/shTERT could effectively inhibit the tumor growth and induce cell apoptosis of OC, while showing good targeting and in vivo safety. We believe that this study can provide new safe and effective ideas for the current clinical treatment of OC.

Abbreviations

ALP	Alkaline phosphatase
ALT	Serum alanine aminotransferase
AST	Aspartate aminotransferase
BUN	Urea nitrogen
CDK	Cyclin-dependent kinase
MSN	Mesoporous silicon dioxide
OC	Ovarian cancer
PLT	Platelet
QR	Quercetin
RBC	Red blood cell
TBIL	Total bilirubin
TERT	Telomerase reverse transcriptase
TR	Telomerase RNA
WBC	White blood cell

Supplementary Information

The online version contains supplementary material available at <https://doi.org/10.1186/s12951-025-03546-0>.

Supplementary file 1.

Acknowledgements

We thank all authors who contributed valuable methods and data and made them public.

Author contributions

M. L. conceived and designed this study. G. C., W. S., W. X., W. H., R. D., and G. M. Performed experiments and/or analyzed data and/or prepared the figures. G. C., W. S. and G. M. analyzed data. G. C and Y. Z. wrote the first version of the manuscript. H. Z., Y. H. and M. L. revised the manuscript. X. F. and M. L. funded this research. All authors have read and approved the final manuscript. We thank all authors who contributed valuable methods and data and made them public.

Funding

This work was supported by Social Development Plan of Taizhou, China (Grant No.TS202419),The 333 Plan Foundation of Jiangsu, China (Grant No. [2022] 21–2) and Suqian Sci & Tech Program (Grant No.KY202212).

Data availability

No datasets were generated or analysed during the current study.

Declarations

Ethics approval and consent to participate

All animal experiments complied with the ARRIVE guidelines and were carried out in accordance with the National Research Council's Guide for the Care and Use of Laboratory Animals. The animal experimental protocols in this study were approved by the Huachuang Sino Animal Experiment Ethics Committee (SK23035-P001-01).

Consent for publication

Not applicable.

Competing interests

The authors declare no competing interests.

Author details

¹Clinical Laboratory, Affiliated Taizhou People's Hospital of Nanjing Medical University, Taizhou 225300, Jiangsu, People's Republic of China. ²Medical School of Nantong University, Nantong 226001, Jiangsu, People's Republic of China. ³Nanjing University of Chinese Medicine, Nanjing 210023, Jiangsu, People's Republic of China. ⁴Department of Endocrinology, Nantong First People's Hospital, Nantong 226001, Jiangsu, People's Republic of China. ⁵Department of Neurosurgery, The Affiliated Hospital of Xuzhou Medical University, Xuzhou 221000, Jiangsu, People's Republic of China. ⁶Department of Neurosurgery, The Affiliated Suqian First People's Hospital of Nanjing Medical University, Suqian 223800, Jiangsu, People's Republic of China.

Received: 12 March 2025 Accepted: 12 June 2025

Published online: 22 July 2025

References

- Bray F, Laversanne M, Sung H, Ferlay J, Siegel RL, Soerjomataram I, Jemal A. Global cancer statistics 2022: GLOBOCAN estimates of incidence and mortality worldwide for 36 cancers in 185 countries. *CA Cancer J Clin*. 2024;74(3):229–63.
- Hinchcliff E, Westin SN, Herzog TJ. State of the science: contemporary front-line treatment of advanced ovarian cancer. *Gynecol Oncol*. 2022;166(1):18–24.
- Zapardiel I, Diestro MD, Aletti G. Conservative treatment of early stage ovarian cancer: oncological and fertility outcomes. *Eur J Surg Oncol*. 2014;40(4):387–93.
- Li Y, Wicha MS, Schwartz SJ, Sun D. Implications of cancer stem cell theory for cancer chemoprevention by natural dietary compounds. *J Nutr Biochem*. 2011;22(9):799–806.
- Cianciosi D, Varela-Lopez A, Forbes-Hernandez TY, Gasparrini M, Afrin S, Reboredo-Rodriguez P, Zhang J, Quiles JL, Nabavi SF, Battino M, et al.

- Targeting molecular pathways in cancer stem cells by natural bioactive compounds. *Pharmacol Res.* 2018;135:150–65.
6. Rauf A, Imran M, Khan IA, Ur-Rehman M, Gilani SA, Mehmood Z, Mubarak MS. Anticancer potential of quercetin: a comprehensive review. *Phytother Res.* 2018;32(11):2109–30.
 7. Iacopetta D, Grande F, Caruso A, Mordocco RA, Plutino MR, Scrivano L, Ceramella J, Muià N, Saturnino C, Puoci F, et al. New insights for the use of quercetin analogs in cancer treatment. *Future Med Chem.* 2017;9(17):2011–28.
 8. Yi L, Zongyuan Y, Cheng G, Lingyun Z, Guilian Y, Wei G. Quercetin enhances apoptotic effect of tumor necrosis factor-related apoptosis-inducing ligand (TRAIL) in ovarian cancer cells through reactive oxygen species (ROS) mediated CCAAT enhancer-binding protein homologous protein (CHOP)-death receptor 5 pathway. *Cancer Sci.* 2014;105(5):520–7.
 9. Brito AF, Ribeiro M, Abrantes AM, Pires AS, Teixo RJ, Tralhão JG, Botelho MF. Quercetin in cancer treatment, alone or in combination with conventional therapeutics? *Curr Med Chem.* 2015;22(26):3025–39.
 10. Daniel M, Peek GW, Tollefsbol TO. Regulation of the human catalytic subunit of telomerase (hTERT). *Gene.* 2012;498(2):135–46.
 11. Ramlee MK, Wang J, Toh WX, Li S. Transcription regulation of the human telomerase reverse transcriptase (hTERT) gene. *Genes (Basel).* 2016;7(8):50.
 12. Saretzki G. Extra-telomeric functions of human telomerase: cancer, mitochondria and oxidative stress. *Curr Pharm Des.* 2014;20(41):6386–403.
 13. Cong YS, Wright WE, Shay JW. Human telomerase and its regulation. *Microbiol Mol Biol Rev.* 2002;66(3):407–25.
 14. Ivancich M, Schrank Z, Wojdyła L, Leviskas B, Kuckovic A, Sanjali A, Puri N. Treating cancer by targeting telomeres and telomerase. *Antioxidants (Basel).* 2017;6(1):15.
 15. Garbayo E, Pascual-Gil S, Rodríguez-Nogales C, Saludas L, Estella-Hermoso de Mendoza A, Blanco-Prieto MJ. Nanomedicine and drug delivery systems in cancer and regenerative medicine. *Wiley Interdiscip Rev Nanomed Nanobiotechnol.* 2020;12(5): e1637.
 16. Benezra M, Penate-Medina O, Zanzonico PB, Schaer D, Ow H, Burns A, DeStanchina E, Longo V, Herz E, Iyer S, et al. Multimodal silica nanoparticles are effective cancer-targeted probes in a model of human melanoma. *J Clin Invest.* 2011;121(7):2768–80.
 17. He Q, Shi J, Chen F, Zhu M, Zhang L. An anticancer drug delivery system based on surfactant-templated mesoporous silica nanoparticles. *Biomaterials.* 2010;31(12):3335–46.
 18. Zhang M, Kim S, Yang HW. Non-canonical pathway for Rb inactivation and external signaling coordinate cell-cycle entry without CDK4/6 activity. *Nat Commun.* 2023;14(1):7847.
 19. Mrózek A, Petrowsky H, Sturm I, Kraus J, Hermann S, Hauptmann S, Lorenz M, Dörken B, Daniel PT. Combined p53/Bax mutation results in extremely poor prognosis in gastric carcinoma with low microsatellite instability. *Cell Death Differ.* 2003;10(4):461–7.
 20. Martins FC, Couturier DL, de Santiago I, Sauer CM, Vias M, Angelova M, Sanders D, Piskorz A, Hall J, Hosking K, et al. Clonal somatic copy number altered driver events inform drug sensitivity in high-grade serous ovarian cancer. *Nat Commun.* 2022;13(1):6360.
 21. Wang Y, Duval AJ, Adli M, Matei D. Biology-driven therapy advances in high-grade serous ovarian cancer. *J Clin Invest.* 2024;134:1.
 22. Minaei A, Sabzichi M, Ramezani F, Hamishehkar H, Samadi N. Co-delivery with nano-quercetin enhances doxorubicin-mediated cytotoxicity against MCF-7 cells. *Mol Biol Rep.* 2016;43(2):99–105.
 23. Jacquemin G, Granci V, Gallouet AS, Lalaoui N, Morlé A, Iessi E, Morizot A, Garrido C, Guillaudeux T, Micheau O. Quercetin-mediated Mcl-1 and survivin downregulation restores TRAIL-induced apoptosis in non-Hodgkin's lymphoma B cells. *Haematologica.* 2012;97(1):38–46.
 24. Kee JY, Han YH, Kim DS, Mun JG, Park J, Jeong MY, Um JY, Hong SH. Inhibitory effect of quercetin on colorectal lung metastasis through inducing apoptosis, and suppression of metastatic ability. *Phytomedicine.* 2016;23(13):1680–90.
 25. Xingyu Z, Peijie M, Dan P, Youg W, Daojun W, Xinzheng C, Xijun Z, Yangrong S. Quercetin suppresses lung cancer growth by targeting Aurora B kinase. *Cancer Med.* 2016;5(11):3156–65.
 26. Ferry DR, Smith A, Malkhandi J, Fyfe DW, deTakats PG, Anderson D, Baker J, Kerr DJ. Phase I clinical trial of the flavonoid quercetin: pharmacokinetics and evidence for in vivo tyrosine kinase inhibition. *Clin Cancer Res.* 1996;2(4):659–68.
 27. Engeland K. Cell cycle regulation: p53–p21–RB signaling. *Cell Death Differ.* 2022;29(5):946–60.
 28. Yao D, Li C, Rajoka MSR, He Z, Huang J, Wang J, Zhang J. P21-Activated Kinase 1: emerging biological functions and potential therapeutic targets in cancer. *Theranostics.* 2020;10(21):9741–66.
 29. Wiedemuth R, Klink B, Töpfer K, Schröck E, Schackert G, Tatsuka M, Temme A. Survivin safeguards chromosome numbers and protects from aneuploidy independently from p53. *Mol Cancer.* 2014;13:107.
 30. Chiba K, Lorbeer FK, Shain AH, McSwiggen DT, Schruf E, Oh A, Ryu J, Darzacq X, Bastian BC, Hockemeyer D. Mutations in the promoter of the telomerase gene TERT contribute to tumorigenesis by a two-step mechanism. *Science.* 2017;357(6358):1416–20.
 31. Levine AJ, Tomasini R, McKeon FD, Mak TW, Melino G. The p53 family: guardians of maternal reproduction. *Nat Rev Mol Cell Biol.* 2011;12(4):259–65.
 32. Meng H, Xue M, Xia T, Ji Z, Tarn DY, Zink JI, Nel AE. Use of size and a copolymer design feature to improve the biodistribution and the enhanced permeability and retention effect of doxorubicin-loaded mesoporous silica nanoparticles in a murine xenograft tumor model. *ACS Nano.* 2011;5(5):4131–44.
 33. Cheng W, Nie J, Xu L, Liang C, Peng Y, Liu G, Wang T, Mei L, Huang L, Zeng X. pH-sensitive delivery vehicle based on folic acid-conjugated polydopamine-modified mesoporous silica nanoparticles for targeted cancer therapy. *ACS Appl Mater Interfac.* 2017;9(22):18462–73.

Publisher's Note

Springer Nature remains neutral with regard to jurisdictional claims in published maps and institutional affiliations.